The rotational spectrum of $H^{32}SOH$ and $H^{34}SOH$ above 1 THz

Oliver Baum,[1,a)] Monika Koerber,[1] Oliver Ricken,[1] Gisbert Winnewisser,[1] Sergei N. Yurchenko,[2] Stephan Schlemmer,[1] Koichi M. T. Yamada,[3] and Thomas F. Giesen[1]

[1]*I. Physikalisches Institut, Universität zu Köln, Zülpicher Straße 77, D-50937 Köln, Germany*
[2]*Technische Universität Dresden, Institut für Physikalische Chemie und Elektrochemie, D-01062 Dresden, Germany*
[3]*National Institute of Advanced Industrial Science and Technology (AIST), Tsukuba-West 305-8569, Japan*

(Received 8 October 2008; accepted 4 November 2008; published online 12 December 2008)

Accurate spectral data of $H^{32}SOH$ and $H^{34}SOH$ at 1.3 THz were recorded using a synthesizer based multiplier spectrometer. The spectra were analyzed together with data from an earlier study which contain measurements at 1.9 THz. The combination of both data sets allows to determine experimentally the tunneling splitting of energy levels with $K_a=4$ and 5 for the first time. The obtained results are essential to test a novel model on torsional tunneling splitting in HSOH. Transitions with $K_a=1\leftarrow 0$, $K_a=2\leftarrow 1$, and $K_a=3\leftarrow 2$ all exhibit strong *c*-type and somewhat weaker *b*-type transitions. In contrary, transitions with $K_a=4\leftarrow 3$ display only *c*-type but no *b*-type transitions. The absence of *b*-type transitions is completely unexpected and yet not well understood. For the $H^{34}SOH$ isotopolog the data set has been substantially extended by the new measurements of ${}^rQ_3$-branch transitions at 1.3 THz. Based on the new data the accuracy of the $H^{34}SOH$ molecular parameters has been significantly improved. © *2008 American Institute of Physics*.
[DOI: 10.1063/1.3034741]

I. INTRODUCTION

In 2003 Winnewisser *et al.*[1] reported the unequivocal gas-phase detection of HSOH by means of its rotational spectrum. Further investigations on HSOH and its isotopologs,[1–6] as well as highly accurate *ab initio* calculations,[7] have substantially improved our knowledge on this peculiar molecule.

HSOH can be considered as a link between two well known homonuclear species, HSSH (Ref. 8) and HOOH (Ref. 9). Molecules of type XYYX (with X=H,D and Y=S,O) have two equivalent equilibrium conformations which are the most simple representatives of molecular enantiomers. Tunneling between the two corresponding potential energy minima, which is classically an internal rotation (torsion) about the heavy atom bond YY, causes rotational transitions to split into doublets. This tunneling splitting is well studied for HSSH and HOOH. The observed splitting depends on both the height of the potential barrier and the K_a projection quantum number of the total angular momentum J. K_a is almost a good quantum number because the molecules of type XYYX are very close symmetric prolate tops.

In the cases of HSSH and HOOH it was found that the size of the splitting alternates with K_a in modulo 2.[8,9] This phenomenon has been described in a theoretical model introduced by Hougen[10] and Hougen and DeKoven,[11] which is in good agreement with the experiment. HSOH is of lower symmetry than the C_2 molecules HSSH and HOOH; hence, the tunneling splitting is found to be a more complicated function of K_a, which was the subject of a recent theoretical treatment by Yamada *et al.*[12] Their model is presented in terms of a relatively simple parametrized form of the internal rotation dynamics in HSOH. It predicts a variation of the energy level splitting due to the tunneling which is the largest and almost identical in the cases of $K_a=0,3,6,\ldots$. This is in agreement with the experimentally derived quantities of 64.5 and 62.9 MHz for $K_a=0$ and $K_a=3$, respectively.

The purpose of the present studies is mainly twofold: (a) to determine the torsional splitting of $K_a=4$ and $K_a=5$ energy levels experimentally for testing recently published high level *ab initio* calculations on tunneling splitting in HSOH by Ovsyannikov *et al.*[7] and (b) to give precise data for improved molecular parameters on the ^{32}S and ^{34}S main isotopologs of HSOH. Compared to the ^{32}S main isotopolog, spectral data on the ^{34}S species are rather sparse. Nevertheless, due to the high sensitivity of the 1.3 THz multiplier spectrometer employed for the present measurements, spectra of $H^{34}SOH$ were recorded in natural abundance.

The measurements presented here exhibit an unexpected effect, namely, all *b*-type transitions are missing in the ${}^rQ_3$ branch.

The results of these studies and their analysis are presented in this paper, which is organized as follows. In Sec. II we present the spectrometers used for measurements at 1.3 and 1.9 THz, with emphasis on the new multiplier spectrometer at 1.3 THz. Details on the recorded $H^{32}SOH$ and $H^{34}SOH$ spectra and the data analysis including previous measurements are given in Sec. III. The tunneling splittings of $K_a=4$ and $K_a=5$ levels have been derived from combination differences and are compared to recently improved *ab initio* calculations in Sec. IV. The molecular parameters derived from these highly accurate measurements allow to pre-

a)Electronic mail: baum@ph1.uni-koeln.de.

dict line positions of *b*-type transitions of the ${}^{r}Q_3$ branch within less than 50 kHz. Nevertheless not a single *b*-type transition has been recorded. This unexpected finding of missing transitions is discussed in Sec. V.

II. EXPERIMENTAL SETUP

At the Cologne laboratories the spectral range up to 1 THz is covered by frequency stabilized spectrometers using backward wave oscillators (BWOs) as monochromatic radiation sources.[13] To record spectra above 1 THz new high frequency techniques have been applied and further developed. At 1.3 THz the 72nd harmonic of an 18 GHz synthesizer signal (Agilent, Inc.), generated in a commercially available multiplier chain (Virginia Diodes, Inc.), is used. Details of the employed multiplier chain are given in Refs. 14 and 15. Briefly, a primary frequency doubler is followed by an amplifier to enhance the output power. A quadrupler and two succeeding triplers are used for further multiplication which finally generate a factor of 72 of the 18 GHz synthesizer fundamental frequency. The multiplier device has been designed for output powers of about 1 μW with a maximum of broadband tunability. The terahertz output signal is scanned over several gigahertz (4 GHz in this case) by continuously tuning the synthesizer frequency. High frequency accuracy is obtained by phase locking the synthesizer frequency to a rubidium time standard which has a stability $\Delta\nu/\nu$ of 10^{-11}. A personal computer is used to scan the frequency of the spectrometer and to record the signal from a lock-in amplifier in second derivative. For sensitive detection of the 1.3 THz signal an InSb hot electron bolometer cooled to liquid Helium temperature is employed.

Data from $K_a=5\leftarrow4$ transitions of an earlier work,[1] which were recorded employing the COlogne Sideband Spectrometer for Terahertz Applications (COSSTA), have been used to determine the tunneling splitting of the $K_a=5$ levels. COSSTA combines the fix frequency of a far-infrared gas laser at 1.9 THz with a tunable output frequency of a 300 GHz BWO. Details of the spectrometer were published by Lewen *et al.*[16]

Gas-phase HSOH is not stable under usual laboratory conditions and thus the molecule was produced *in situ* under a constant gas flow. Referring to earlier investigations it turned out that among different pathways of producing HSOH, flash vacuum pyrolysis of di-*tert*-butyl sulfoxide is the most efficient one.[1,6,17] The lifetime of HSOH is of the order of a few seconds which required a constant flow of a fresh sample through the 3 m long absorption cell.

III. THE ${}^{r}Q_3$ BRANCH OF HSOH AND ITS ISOTOPOLOG $H^{34}SOH$

The permanent electrical dipole moment of HSOH is pointing almost perpendicular to the S–O bond and toward the angle bisector of the dihedral angle. Hence, a perpendicular-type spectrum is observed which exhibits strong *Q* branches at distances $(A-(B+C)/2)(2K_a+1)$, with *A*, *B*, and *C* the rotational constants and K_a the projection of the angular momentum onto the symmetry axis. The ${}^{r}Q_{K''_a=0,1,2}$ branches of HSOH occur at 187, 561, and 935 GHz, respectively. Molecular constants from a previous study[1] have been used to predict line positions of the ${}^{r}Q_3$ branch occurring at 1.308 THz, which leads to a clear identification of the current spectra in the region between 1.295 and 1.308 THz.

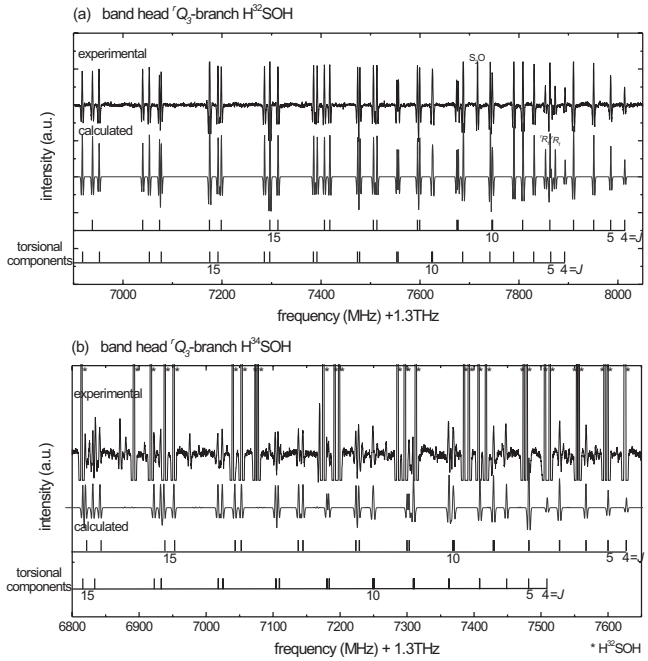

FIG. 1. Band head of the ${}^{r}Q_3$ branch of (a) HSOH and (b) its isotopolog $H^{34}SOH$. In each case the experimental spectrum is depicted in the upper trace, while a calculated spectrum based on the molecular parameters of the final data analysis is plotted in the lower trace. Each transition is split by two effects: (i) the torsional splitting due to the internal rotation in HSOH and (ii) the splitting due to the internal asymmetry of the molecule. The assignment of each transition to the corresponding torsional component is given. The asymmetry splitting of individual transitions is clearly seen for transitions with $J>10$.

A part of the ${}^{r}Q_3$ band head spectrum of $H^{32}SOH$ at 1.308 THz is depicted in the upper trace of Fig. 1(a). The tunnel effect splits rotational transition into two components, which in the case of the ${}^{r}Q_3$ branch are found to be separated by 120 MHz. The stick diagrams in Fig. 1 show the assignment of *c*-type rotational transitions to the quantum numbers *J* of both tunnel components. As can be seen from the graph, the tunneling splitting is almost *J* independent. Furthermore, each rotational transition splits into a doublet due to the internal asymmetry, which in the case of HSOH is small because of almost identical *B* and *C* rotational constants. Progression of the asymmetry splitting with increasing *J* quantum numbers can be best seen from the stick diagram in Fig. 1(a). All lines of the ${}^{r}Q_3$ branch up to $J=40$ have been assigned.

Corresponding to their isotopic ratio, transitions of the $H^{34}SOH$ isotopolog are weaker by a factor of 20 than the $H^{32}SOH$ transitions. The high sensitivity of the spectrometer made it possible to record 36 transitions of the $H^{34}SOH$ ${}^{r}Q_3$ branch in natural abundance. Figure 1(b) shows the ${}^{r}Q_3$ branch spectrum at a magnified scale.

In Fig. 2 the Fortrat diagrams for (a) $H^{32}SOH$ and (b) $H^{34}SOH$ are displayed from 0 to 2 THz, showing the positions of *Q* branches with $K''_a=0,\ldots,4$. Details on ${}^{r}Q_3$

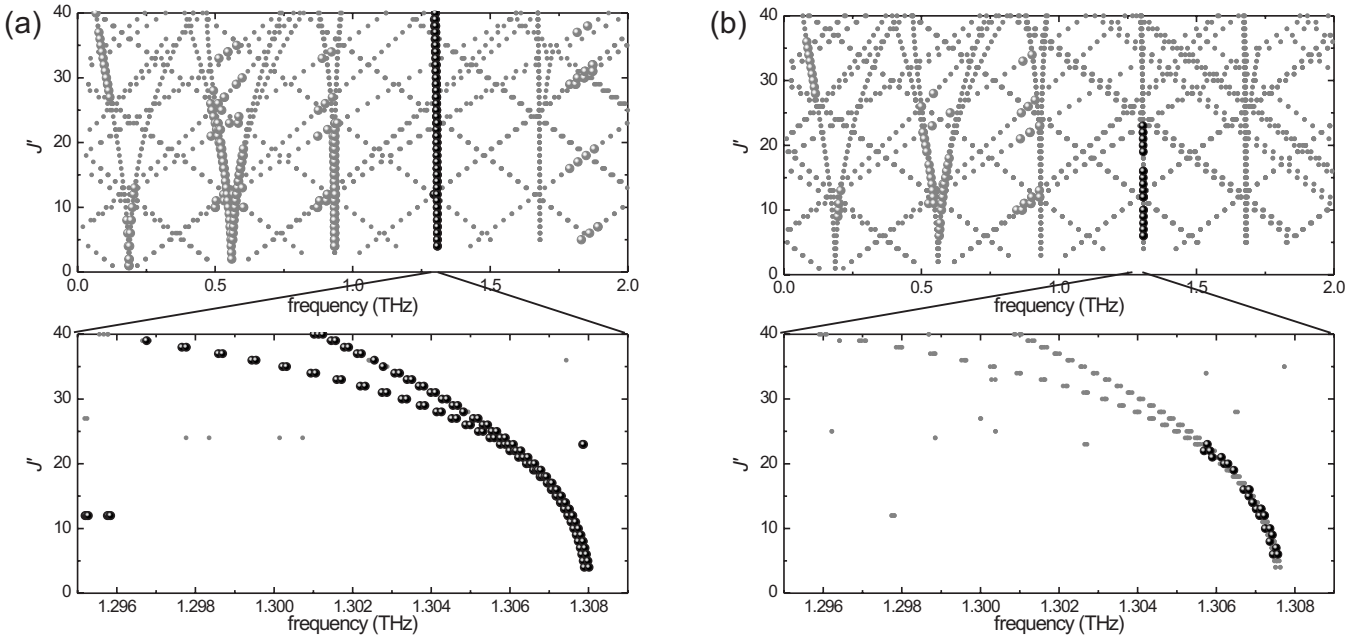

FIG. 2. Fortrat diagram of (a) HSOH and its isotopolog (b) $H^{34}SOH$. Experimentally assigned lines are marked by circles [gray (Ref. 1) and black (this work)]. The blow-ups in the lower traces show the details of the ${}^rQ_3$-band center regions at 1.308 THz.

branches studied here are depicted in Figs. 2(a) and 2(b); the lower traces show the details. All new lines assigned in the course of this work are marked with black dots, while lines measured in previous work[1] are marked with gray dots.

For the main isotopolog $H^{32}SOH$ the data set now contains 617 assigned transitions in total, from which 142 lines at 1.3 THz were added in the present work. All new data were recorded using the 1.3 THz multiplier spectrometer described in Sec. II. In the analysis 132 of the 142 measured lines were assigned to the ${}^rQ_3$ branch, 8 to the ${}^rR_2$ branch, and 2 to ${}^rR_1$ branch transitions of $H^{32}SOH$. All 617 transitions were finally analyzed in a global fit and improved parameters were obtained from fitting the data to a Watson Hamiltonian in *S* reduction by employing Pickett's program SPFIT.[18] To account for torsional splitting and interaction of the torsional substates, a two-state fit has been used. This fit is successful for all lines up to the $K_a=5\leftarrow4$ transitions at 1.9 THz.[19] Figure 3 shows the two components of tunneling

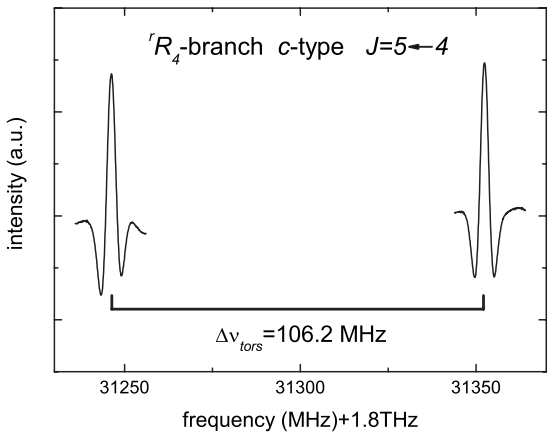

FIG. 3. The observed $J=5\leftarrow4$ *c*-type transitions of the ${}^rR_4$ branch indicate a torsional splitting of 106 MHz.

splitting for the $J=5\leftarrow4$ *c*-type transition in the ${}^rR_4$ branch at 1.83 THz.

As can be seen from the Fortrat diagram in Fig. 2(b) the data set of $H^{34}SOH$ is less complete compared with the main isotopolog. It contains 116 transitions up to 930 GHz. Since transitions above 1 THz were completely missing, the 36 new assigned ${}^rQ_3$ branch transitions at 1.3 THz presented here led to a substantial improvement of the $H^{34}SOH$ data set. Molecular constants obtained from a global analysis of all $H^{32}SOH$ and $H^{34}SOH$ transitions are listed in Table I.

IV. INTERNAL ROTATION TUNNELING IN HSOH

The spectra of HSOH and its isotopologs exhibit a splitting of rotational transitions which is caused by the internal rotation tunneling motion. The splitting is observed for all transitions in HSOH and found to be clearly K_a dependent. Furthermore, the splitting also depends on *J*, especially for the ${}^rQ_1$ and ${}^rQ_2$ branches, as can be seen from Fig. 4. Because of the strong nonlinear *J* dependence in the low-*J* region, the rotational splittings $\Delta\nu(b)$ and $\Delta\nu(c)$ reported by Yamada *et al.*[12] were determined for $J\approx10$ transitions (see Fig. 4) and assumed to be the same value for $J\rightarrow0$. For comparison with new *ab initio* calculations presented by Ovsyannikov *et al.*[7] we report here revised rotation splitting parameters $\Delta\nu(b)$ and $\Delta\nu(c)$, which take the strong nonlinear *J* dependence into account (see Table II). In Fig. 4 experimental values of $\Delta\nu(b)$ and $\Delta\nu(c)$ (black circles) as well as expected transition splittings (gray dots), based on the best fit parameters, are plotted. By this manner the splitting values for the minimum *J* of each ${}^rQ_{K_a}$ branch have been evaluated. The revised values for the minimum *J* of the internal rotation splitting observed in the transitions of the ${}^rQ_{K_a}$ branches ($K_a=0,1,2,3$) and the ${}^rR_4$ branch of HSOH are listed in Table II. From the measured splittings $\Delta\nu(b)_{K_a}$ and $\Delta\nu(c)_{K_a}$

TABLE I. Ground state molecular parameters (MHz) of H ^{32}SOH and H ^{34}SOH.

Parameter	H ^{32}SOH	H ^{34}SOH
A	202069.04977(109)	201 739.7555(172)
$\Delta A/2$	−14.3854(36)	−12.867(75)
B	15281.956049(115)	15001.43857(64)
$\Delta B/2\times10^3$	−2.8370(91)	−2.698(53)
C	14840.215513(114)	14573.77800(58)
$\Delta C/2\times10^3$	4.3369(51)	4.196(48)
$D_J\times10^3$	24.528141(132)	23.68948(100)
$\Delta D_J/2\times10^6$	0.33926(312)	0.316(46)
D_{JK}	0.39036280(308)	0.378836(53)
$\Delta D_{JK}/2\times10^3$	0.2529(35)	0.441(43)
D_K	5.990400(144)	5.9663(34)
$\Delta D_K/2$	−1.07509(127)	−0.732(97)
$d_1\times10^3$	−0.7163957(173)	−0.681564(229)
$d_2\times10^3$	0.2910757(96)	0.270416(280)
$\Delta d_2/2\times10^6$	0.3163(40)	0.187(78)
$H_J\times10^6$	−0.015185(37)	−0.01454(55)
$H_{JK}\times10^6$	−1.27430(217)	−1.087(62)
$\Delta H_{JK}/2\times10^6$	0.02738(138)	−0.069(54)
$H_{KJ}\times10^3$	0.029521(109)	0.0262(33)
$\Delta H_{KJ}/2\times10^3$	0.01037(39)	0.0593(34)
$H_K\times10^3$	0.5712(55)	0.474(141)
$\Delta H_K/2\times10^6$	−0.031066(153)	0.4122(244)
$h_1\times10^9$	1.1071(68)	0.928(224)
$h_2\times10^9$	−1.4939(54)	−0.86(67)
$h_3\times10^9$	−0.9146(71)	2.31(172)
$\Delta L_K/2\times10^3$	0.3814(60)	−0.01984(121)
ΔE	64.5226(59)	64.1904(279)
G_a	−27.306(38)	−27.306 [a]
$G_{aJ}\times10^3$	−0.384(53)	−0.384 [a]
$G_{aJK}\times10^3$	0.0245(39)	0.0245 [a]
G_{aK}	4.8422(156)	4.8422 [a]
G_{aKK}	−0.26984(169)	−0.26984 [a]
$G_{aKKK}\times10^3$	3.751(46)	3.751[a]

[a]Fixed in the analysis to the values of H ^{32}SOH.

of b- and c-type transitions the splitting δ_{K_a} of energy levels can be obtained using

$$\Delta\nu(b)_{K_a} = |\delta_{K_a} - \delta_{K_a+1}|, \quad (1)$$

$$\Delta\nu(c)_{K_a} = \delta_{K_a} + \delta_{K_a+1}, \quad (2)$$

with $K_a=0,1,2,3,\ldots$. Details of the theoretical description can be found in Ref. 12. The values obtained for the energy level splitting (for the minimum J) are summarized in Table III. Recently Ovsyannikov *et al.*[7] calculated the torsional splitting of HSOH by employing a newly computed *ab initio* potential energy surface together with the program TROVE.[20] The splittings obtained by this approach are in excellent agreement with the experimental results presented here (see Table III).

V. INTENSITY ANOMALY IN *b*-TYPE TRANSITIONS OF HSOH

The HSOH molecule is expected to display a rotational spectrum in the vibrational ground state with extremely weak a-type transitions and a dominating perpendicular-type spectrum with strong c-type and somewhat weaker accompanying b-type transitions, as can be understood from theoretical values of the dipole moment components $\mu_a=0.044$ D, $\mu_b=0.77$ D, and $\mu_c=1.43$ D [CCSD(T)/cc-pCVTZ, see Ref. 1)]. Surprisingly, no b-type transitions have been observed for the $^rQ_3$ branch presented here.

In Fig. 1 the band head of the $^rQ_3$ branch of HSOH is depicted and the assignment of the lines to c-type transitions is given via the stick spectrum. In the calculated spectrum shown in the lower traces of Fig. 1(a) b-type transitions have been ignored. The excellent agreement of the experimental and the calculated spectrum shows the high quality of the molecular parameter set given in Table I. By using these rotational constants, the frequencies of the corresponding b-type transitions in the $^rQ_3$ branch ($J\leq30$) can be predicted with an accuracy of at least 50 kHz. According to the calculated values for the permanent dipole moment components, the intensity of b-type transitions is expected to be about four times weaker than the corresponding c-type transitions shown in Fig. 1(a), but they should be five times stronger compared to c-type transitions of H^{34}SOH depicted in Fig. 1(b). This allows only for the conclusion that no b-type transitions occur in the $^rQ_3$ branch or they are by more than one order of magnitude less intense than expected.

Triggered by this unexpected result the intensities of b- and c-type transitions reported previously,[1] i.e., $^rQ_0$, $^rQ_1$, and $^rQ_2$ branches, have been re-examined. In Fig. 5(a) the observed spectra in the band head region of the $^rQ_2$ branch of HSOH is compared with the simulated one. In parts (b) and (c) of this figure the simulated spectra of the b-type and c-type transitions are plotted, respectively, together with the Fortrat diagrams showing the assignments. The excellent agreement between the calculated and the experimental spectrum shown in Fig. 5(a) is obtained by adjusting the intensity ratio S_b/S_c of b- and c-type transitions, respectively, to a value of 0.58, where S_b represents the intensity of a b-type transition and S_c the intensity of a c-type transition of the same J. The calculated spectrum in (a) is the superposition of the two calculated hybrid bands belonging to b- and c-type transitions. It should be noted that the measured intensities of the b- and c-type transitions in the $^rQ_2$ branch are of the same order.

In Table IV the averaged ratios S_b/S_c of the observed intensities are given for the $^rQ_0$, $^rQ_1$, $^rQ_2$, and $^rQ_3$ branches. Although all spectra of Q-branch transitions have been measured in second derivative ($2f$ mode), the relative intensities obtained by the $2f$-mode spectra are almost proportional to those by the $0f$ mode, i.e., true relative intensity. To take into account the different populations of energy levels, the ratio S_b/S_c has been calculated only if the corresponding (involving the same quantum number J) b- and c-type transitions were available. The ratio S_b/S_c presented in Table IV given for a $^rQ_{K_a}$ branch is the average value of all ratios $S_b/S_c|_J$ available. The intensity ratios S_b/S_c observed in the case of the $^rQ_0$ and $^rQ_1$ branches, respectively, are well explained by the permanent dipole moment components. Nevertheless, the value of $S_b/S_c=0.58$ for transitions with $K_a=3\leftarrow2$ as well as the missing b-type transitions in the case of the $^rQ_3$ branch

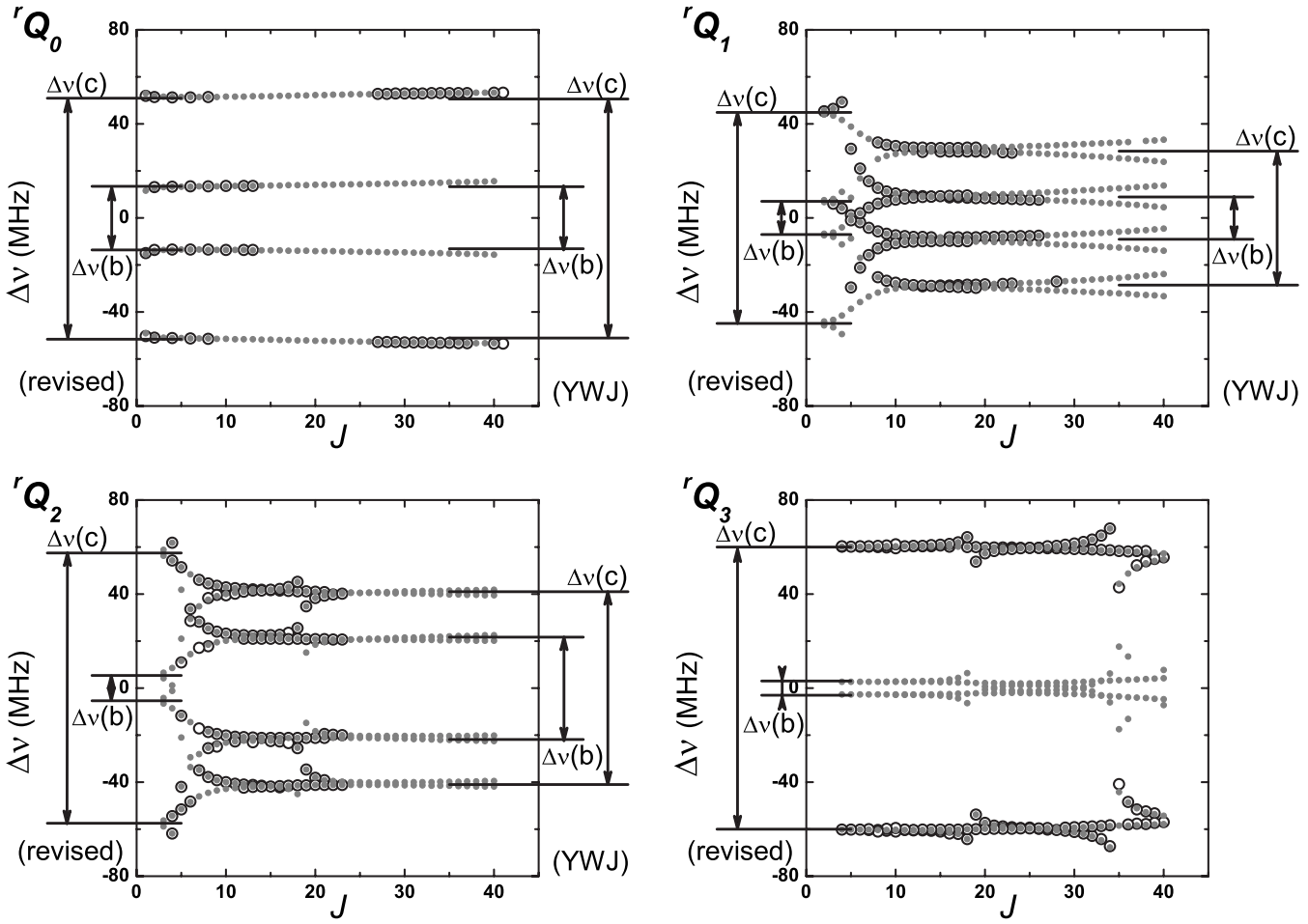

FIG. 4. Torsional splitting for *b*- and *c*-type transitions of the ${}^rQ_{K_a}$ branches are plotted for $K_a=0,1,2,3$. To the right of each diagram the values given in Ref. 12 are indicated, whereas the revised values given in this work are shown on the left. Experimentally assigned transitions are marked by circles.

are completely unexpected. A slightly larger error was obtained for S_b/S_c of the ${}^rQ_2$ branch because of the relatively strong J dependence of the intensity ratio.

VI. CONCLUSION

An active multiplier chain has been introduced to perform high resolution spectroscopy on HSOH at 1.3 THz for the first time. The spectra in Fig. 1 indicate the high quality of the entire experimental setup that has been employed. The measurements presented here are the highest in frequency for the isotopolog $H^{34}SOH$ so far, and thus the accuracy of the rotational parameters was improved significantly. In Table I all results of the fit are summarized. Besides the excellent refinement of the $H^{34}SOH$ data set, also the fit on the $H^{32}SOH$ parameters has been improved.

The measurements on $K_a=4\leftarrow3$ transitions presented here bridge the gap to previously reported measurements[1] on $K_a=5\leftarrow4$ transitions. Hence, it became possible to experimentally determine the torsional splitting for energy levels with $K_a=4$ and 5 for the first time. Furthermore, the highly precise molecular constants allowed us to calculate accurate transition splittings for $K_a=1\leftarrow0$, $K_a=2\leftarrow1$, $K_a=3\leftarrow2$, and

TABLE II. Experimental tunneling splittings of transitions (in MHz).

	$\Delta\nu(c)$		$\Delta\nu(b)$	
Branch	Ref. 12	This work	Ref. 12	This work
${}^rQ_0$	102.0	102.0	26.6	27.0
${}^rQ_1$	57.0	89.8	18.0	14.2
${}^rQ_2$	82.0	115.0	43.5	10.8
${}^rQ_3$		120.0		... [a]
${}^rR_4$		106.2		... [b]

[a]No *b*-type transitions have been observed in this work. For details see Sec. V.
[b]No data on *b*-type transitions are available from the previous work (Ref. 1).

TABLE III. Observed and calculated internal rotation splittings δ_{K_a} (MHz) for energy levels with $K_a=0,\ldots,5$.

	δ_{K_a}	
K_a	Experimental (this work)[a]	Theoretical (Ref. 7)
0	64.5	64.5
1	37.8	37.9
2	52.1	55.3
3	62.9	64.0
4	57.2	58.8
5	49.0	52.9

[a]Obtained by extrapolating the J-dependent splittings of the individual states to the minimum value of J for each level.

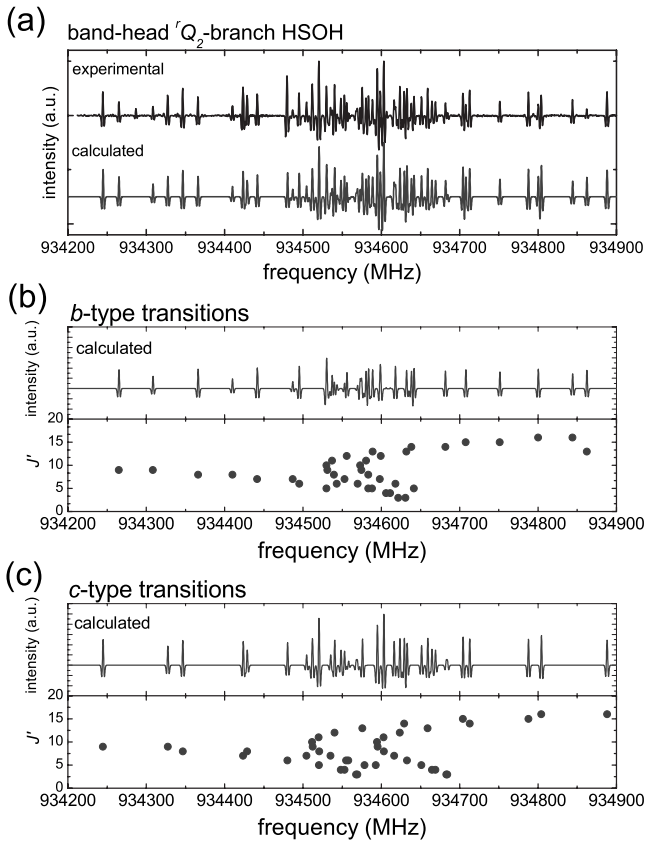

FIG. 5. The intensity of the $^rQ_2$ branch of HSOH was reinvestigated. In (a) the experimental spectrum and a calculated spectrum (based on the constants of the final data analysis) are compared. In (b) and (c) calculated spectra of the *b*- and *c*-type transitions, respectively, are shown separately. In order to get the best agreement between the experimental and calculated spectra, the intensity ratio S_b/S_c has been adjusted to the value of 0.58. The assignment of individual transitions is given via the corresponding Fortrat diagrams.

$K_a=4\leftarrow3$ (see Fig. 4). With the help of these values the torsional splittings reported by Yamada *et al.*[12] have been revised. Since we know the K dependence of the torsional splitting qualitatively,[12] we expect the torsional splitting δ_6 for the $K_a=6$ state to be similar to that of $K_a=3$ (δ_3), say, $\delta_6=58(4)$ MHz at a guess considering that the value of δ_3 is observed to be slightly smaller than the one of δ_0. The experimental proof of this may be one of the most interesting projects in the near future.

The intensity ratios S_b/S_c within the $^rQ_0$, $^rQ_1$, $^rQ_2$, and $^rQ_3$ branches are found to exhibit an anomalous behavior. Usually the intensity ratio S_b/S_c in a b,c-hybrid band should be independent of the K_a quantum number involved and proportional to the corresponding dipole moment component squared. Nevertheless, a strong K_a dependence has been observed in the measurements on HSOH presented here (see Table IV). A detailed discussion on the observed intensity anomaly will be given in a forthcoming paper. Briefly, preliminary results show the observed intensity anomalies to be related to state mixing, i.e., the torsional tunneling effect mixes the state of different K_c levels due to the low symmetry, C_1, of the molecule. Hence, it indicates that in the symmetric top limit ($K_a\geq3$) the intensity of *b*-type transitions vanishes accidentally for HSOH in the ground vibrational state. From the experimental point of view, it is very interesting to check the intensity of *b*-type transitions for higher K_a, i.e., ^rQ_K with $K\geq4$, which is undoubtedly a target for future experiments.

TABLE IV. Experimental intensity ratios S_b/S_c of *b*- and *c*-type transitions in the $^rQ_{K_a}$ branches ($K_a=0,1,2,3$).

Branch	S_b/S_c [a]
$^rQ_0$	0.22(4)
$^rQ_1$	0.23(2)
$^rQ_2$	0.58(11)
$^rQ_3$	$\ll$0.02

[a] $S_b/S_c=\mu_b^2/\mu_c^2=0.29$ is predicted by CCSD(T)/cc-pCVTZ calculations (see Ref. 1) for all $^rQ_{K_a}$ branches.

ACKNOWLEDGMENTS

The authors thank Y. von Mering and Professor A. Klein for the synthesis of the HSOH precursor. Furthermore we thank Dr. S. Thorwirth and Dr. S. Brünken for providing the HSOH data at 1.8 THz. K.M.T.Y. expresses his sincere thanks to T.F.G. and S.S. for their hospitality during his stay in Cologne. This work has been supported by the European Commission [Contract No. MRTN-CT-2004-512202, "Quantitative Spectroscopy for Atmospheric and Astrophysical Research" (QUASAAR)].

[1] G. Winnewisser, F. Lewen, S. Thorwirth, M. Behnke, J. Hahn, J. Gauss, and E. Herbst, Chem.-Eur. J. **9**, 5501 (2003).
[2] M. Behnke, J. Suhr, S. Thorwirth, F. Lewen, H. Lichau, J. Hahn, J. Gauss, K. M. T. Yamada, and G. Winnewisser, J. Mol. Spectrosc. **221**, 121 (2003).
[3] S. Brünken, M. Behnke, S. Thorwirth, K. M. T. Yamada, T. Giesen, F. Lewen, J. Hahn, and G. Winnewisser, J. Mol. Struct. **742**, 237 (2005).
[4] O. Baum, S. Esser, N. Gierse, S. Brünken, F. Lewen, J. Hahn, J. Gauss, S. Schlemmer, and T. F. Giesen, J. Mol. Struct. **795**, 256 (2006).
[5] O. Baum, T. F. Giesen, and S. Schlemmer, J. Mol. Spectrosc. **247**, 25 (2008).
[6] H. Beckers, S. Esser, T. Metzroth, M. Behnke, H. Willner, J. Gauss, and J. Hahn, Chem.-Eur. J. **12**, 832 (2006).
[7] R. I. Ovsyannikov, V. V. Melnikov, W. Thiel, P. Jensen, O. Baum, T. F. Giesen, and S. N. Yurchenko, J. Chem. Phys. **129**, 154314 (2008).
[8] G. Winnewisser and K. M. T. Yamada, Vib. Spectrosc. **1**, 263 (1991).
[9] G. Pelz, K. M. T. Yamada, and G. Winnewisser, J. Mol. Spectrosc. **159**, 507 (1993).
[10] J. T. Hougen, Can. J. Phys. **62**, 1392 (1984).
[11] J. T. Hougen and B. M. DeKoven, J. Mol. Spectrosc. **98**, 375 (1983).
[12] K. M. T. Yamada, G. Winnewisser, and P. Jensen, J. Mol. Struct. **695–696**, 323 (2004).
[13] G. Winnewisser, Vib. Spectrosc. **8**, 241 (1995).
[14] J. Hesler, D. Porterfield, W. Bishop, T. Crowe, A. Baryshev, R. Hesper, and J. Baselmans, Proceedings of the 16th International Symposium on Space Terahertz Technology, Goteborg, Sweden, 2005 (unpublished).
[15] T. W. Crowe, W. L. Bishop, D. W. Porterfield, J. L. Hesler, and R. M. Weikle, IEEE J. Solid-State Circuits **40**, 2104 (2005).
[16] F. Lewen, E. Michael, R. Gendriesch, J. Stutzki, and G. Winnewisser, J. Mol. Spectrosc. **183**, 207 (1997).
[17] S. Esser, Ph.D. thesis, Universität zu Köln, 2006.
[18] H. M. Pickett, J. Mol. Spectrosc. **148**, 371 (1991).
[19] See EPAPS Document No. E-JCPSA6-129-008847 for experimental transition frequencies of HSOH and their assignments. For more information on EPAPS, see http://www.aip.org/pubservs/epaps.html.
[20] S. N. Yurchenko, W. Thiel, and P. Jensen, J. Mol. Spectrosc. **245**, 126 (2007).